Front. Earth Sci. 2015, 9(3): 449–462
DOI 10.1007/s11707-014-0474-3

RESEARCH ARTICLE

Identification of landslide spatial distribution and susceptibility assessment in relation to topography in the Xi'an Region, Shaanxi Province, China

Jianqi ZHUANG[1,2], Jianbing PENG (✉)[1,2], Javed IQBAL[3,4], Tieming LIU[2], Na LIU[2], Yazhe LI[1], Penghui MA[1]

1 School of Geological Engineering and Surveying of Changan University, Key Laboratory of Western China Mineral Resources and Geological Engineering, Xi'an 710054, China
2 Institute of Geo-hazards Mitigation of Chang'an University, Xi'an 710054, China
3 Institute of Geology and Geophysics, Chinese Academy of Sciences, Beijing 100029, China
4 Department of Earth Sciences, COMSATS Institute of Information Technology, Abbottabad, Pakistan

Abstract Landslides are among the most serious of geohazards in the Xi'an Region, Shaanxi, China, and are responsible for extensive human and property loss. In order to understand the distribution of landslides and assess their associated hazards in this region, we used a combination of frequency analysis, logistic analysis, and Geographic Information System (GIS) analysis, with consideration of the spatial distribution of landslides. Using the GIS approach, the five key factors of surface topography, including slope gradient, topographic wetness index (TWI), height difference, profile curvature and slope aspect, were considered. First, the distribution and frequency of landslides were considered in relation to all of the five factors in each of three sub-regions susceptible to landslides (Qin Mountain, Li Mountain, and Loess Tableland). Secondly, each factor's influence was determined by a logistic regression method, and the relative importance of each of these independent variables was evaluated. Finally, a landslide susceptibility map was generated using GIS tools. Locations that had recorded landslides were used to validate the results of the landslide susceptibility map and the accuracy obtained was above 84%. The validation proved that there is sufficient agreement between the susceptibility map and existing records of landslide occurrences. The logistic regression model produced acceptable results (the areas under the Receiver Operating Characteristics (ROC) curve were 0.865, 0.841, and 0.924 in the Qin Mountain, Li Mountain and Loess Tableland). We are confident that the results of this study can be useful in preliminary planning for land use, particularly for construction work in high-risk areas.

Keywords landslide distribution, susceptibility assessment, logistic model, ROC, Xi'an

1 Introduction

Landslides and debris flow are among the most hazardous consequences of heavy rainfall in mountainous regions (Xu et al., 2010; Liu et al., 2012; Tang et al., 2012; Yune et al., 2013). In such areas, a landslide can occur rapidly with little warning and exert heavy impulsive loads on objects in their paths (Keefer et al. 1987; Iverson. 1997; Cui et al., 2012). Landslide prediction models can be classified as advanced prediction or simple prediction models (Dai et al., 2002; Guzzetti et al., 2006, 2008). The advanced prediction model, which is also known as landslide assessment, is generally based on long-term factors (formation background) (Dai et al., 2001); a simple prediction model is generally based on short-term factors with immediate effects (factors causing geo-hazards directly). Although advanced prediction is an assessment of probability and cannot precisely predict the times of landslide occurrences, it can provide information regarding the areas that are prone to landslides, as well as provide an early warning reference for engineering and construction (Cui et al., 2013). Many methods have been used to assess landslides, including expert evaluation, statistical methods, and mechanical approaches (Dai et al., 2002; Fell et al., 2008; Xu et al., 2012). The statistical method is the most widely used approach used for landslide assessment. This method can overcome the subjectivity of expert evaluation

Received January 6, 2014; accepted May 18, 2014

E-mail: rockfans09@163.com

and the demanding geotechnical data requirements of mechanical approaches and has produced successful results (Dai et al., 2001; Guzzetti et al., 2006; Kayastha, 2012; Xu et al., 2013). However, statistical results are largely dependent on the quality of data and the analysis method used (Dai et al., 2002; Ermini et al., 2005). Data may originate from terrain factors, geological factors, precipitation factors, seismic factors, and/or human activity factors. The methods of analysis commonly used include regression analysis (Bai et al., 2010, 2011), neural network analysis (Ermini et al., 2005), discriminatory analysis (Nandi and Shakoor, 2010), and fuzzy logic analysis (Kayastha, 2012). Causative factors such as soil strength and depth of the water table cannot be measured cost-effectively on a regional scale. Therefore, the mapping of landslide susceptibility using GIS technology has become an important tool among these methods, as it enables the rapid assessment of an area with limited resources, in which only landslide inventories, and topographical and geological maps are required for this method.

The city of Xi'an and its surroundings in Shaanxi Province, China are subjected to frequent landslides. This has led to the continuous and repeated destruction of houses, buildings, roads, waterworks, and waste disposal infrastructure in several districts of the city and surrounding areas (Li, 1992). For example, a storm with heavy rainfall on September 12−17, 2011 resulted in the largest landslide of the current decade along the edge of the tableland, and caused destruction of houses and roads, and the loss of 32 lives. Therefore, accurate landslide assessment has always been a key concern to the regional government. As early as the 1980s, the Geology Environmental Monitoring Station had installed a ''geo-hazard inventory detail'' in this region in order to monitor landslide activity for the purpose of making future predictions.

Unfortunately, passive mitigation measures have not been very successful in preventing landslides. There are two reasons for the failure of landslide prevention; firstly, the measures taken were based on past landslides and the areas that were potentially vulnerable to landslides in the future were not considered. Some of the catastrophic landslides occurred in places that were considered to be safe over several decades. Secondly, the late recognition of the fact that landslides might not only be triggered by precipitation but can also be triggered by human activity has been a contributing factor. The practice of modifying slopes for construction and other engineering activities is unavoidable because of terrain limitations in the area. However, these activities made the slopes steeper and even more susceptible to landslides. This makes the development of landslide susceptibility mapping an important means of predicting landslides and examining the effects of human activity.

In order to reveal the general characteristics of landslides and to assess their potential distribution, it is important to statistically analyze the areas in which landslides have occurred and where there is trend to slope failure. In this study, the logistic regression method is used to predict the potential areas of landslide occurrences, and ROC curve analysis is applied to select the best-fitting model for predicting their potential distribution in the Xi'an Region. Based on these results, the potential distribution is mapped in the study area. Field investigations on the regional topography, as well as the existing literature on the subject were reviewed with respect to landslide occurrences. On these bases, a GIS-based probabilistic analysis approach was developed and applied to evaluate landslides and associated hazards in this region.

2 Area setting

The Xi'an Region, located in central Shaanxi, is a rift basin between the Qin Mountain to the south and a loess plateau to the north (Fig. 1). This rift basin lies between latitudes 33°39′30"N to 34°45′00"N and longitudes 107°39′00"E to 109°49′00"E (Fig. 1). It spans a large area of the Wei River Basin and parts of the Qin Mountain with a total area of about 10,106 km^2. The mean altitude is 1,027 m, with an altitude range from 228 m near Lindong (Wei River Basin) in the east to 3,772 m near Zhouzhi (Qin Mountain) in the west (Fig. 1). The Wei River is the main watercourse from west to east and has several dozen tributaries originating from the Qin Mountain from north to south (Fig. 1). Tectonically, the region is situated at the junction of the Erdos, Ganqing, South China, and North China Blocks. This tectonic setting has resulted in a series of Quaternary thrust faults forming in this region (Li, 1992), including the North Qin Mountain fault, Li Mountain fault, and the Guanshan fault. This indicates that the geological setting of this area is highly complex.

The region can be divided into four geomorphic units according to their topographical and geological features: Qin Mountain (A: Proterozoic and mesozoic granite gneiss), Li Mountain (B: pre Cambrian metamorphic rocks and covered by Quaternary loess), Loess Tableland (C: covered by Malan, Lishi and Wucheng loess) and Wei River Plain (D: Quaternary fluvial sediments and deposit) (Fig. 2).

The Qin Mountain zone, which occupies 50.2% of the region, runs along a west-east axis with a decrease in altitude along this axis. In addition, the north slopes are steeper than the south slopes. Several streams originate from this range and flow from north to south; these streams have gradually eroded the mountains and created the rolling topography characteristic of this region. The average slope of the Qin Mountain in this region is 27.8°, with a range from 76.9° to 12.8°. The Qin Mountain

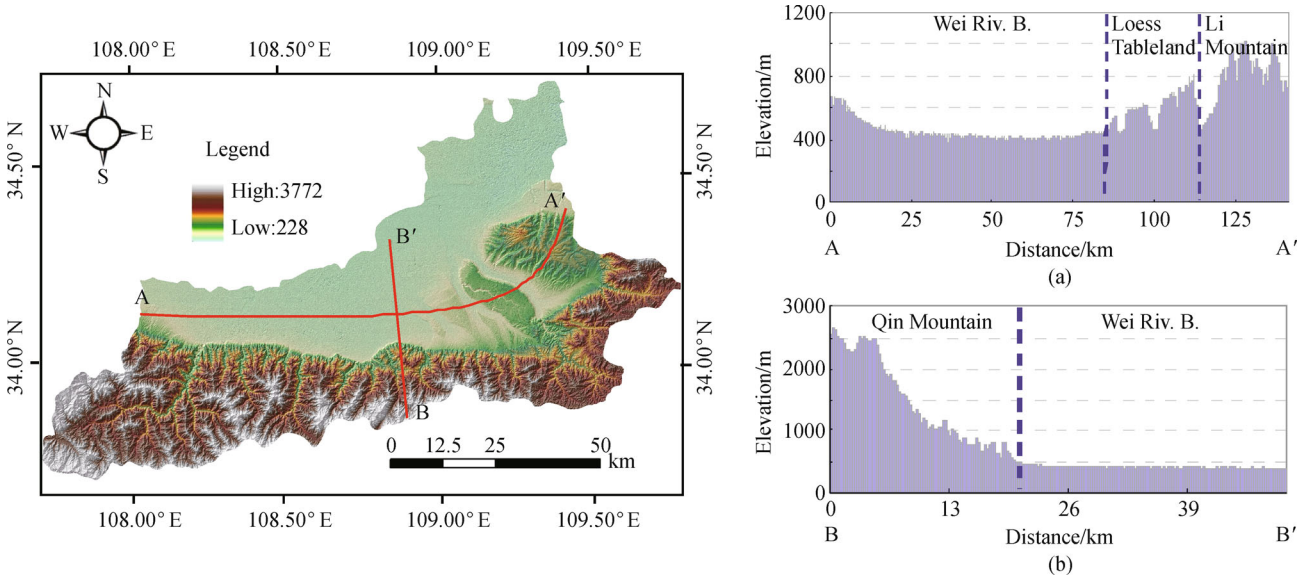

Fig. 1 Landform characteristics of the Xi'an Region (left) and landform cross-section (right); (a) A−A′ cross-section; (b) B−B′ cross-section.

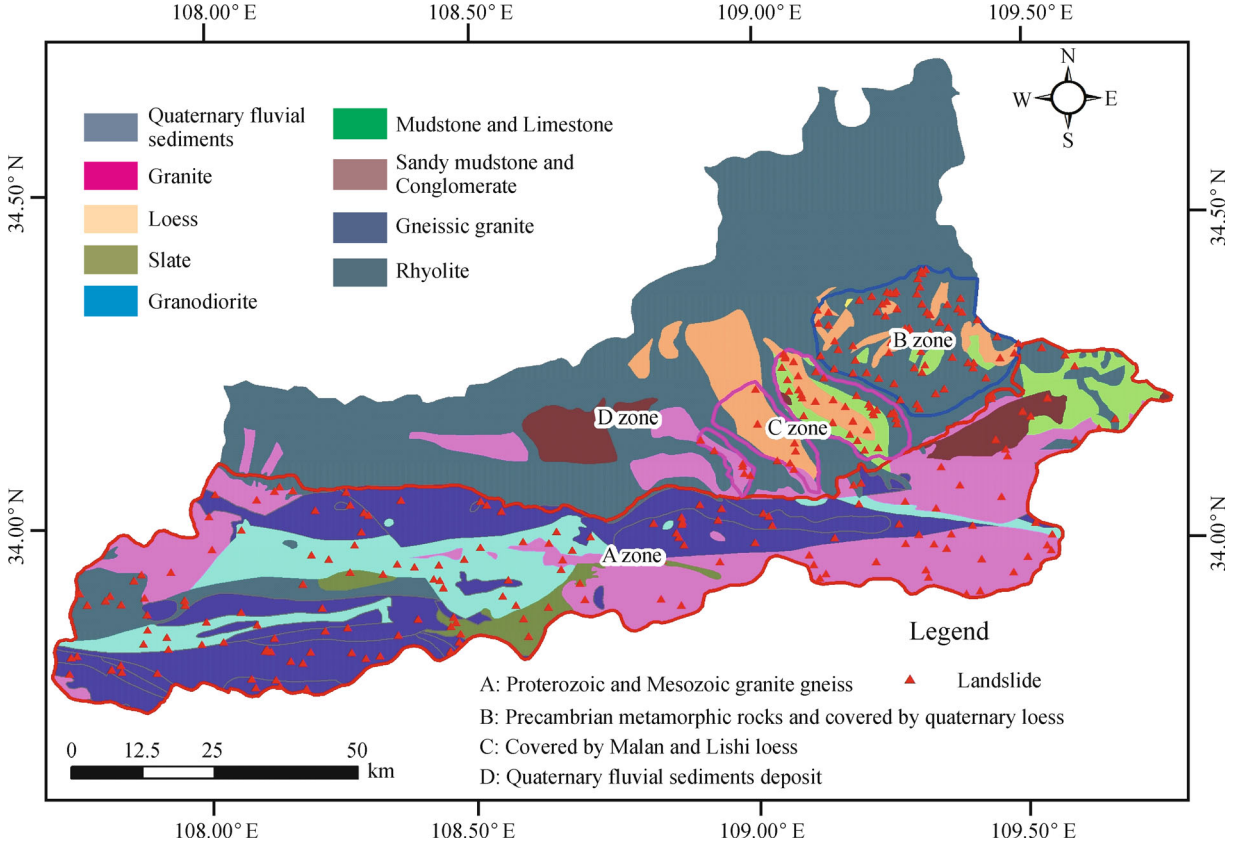

Fig. 2 Simplified geological map of the four sub-regions in Xi'an, China.

uplift is located at the footwall of the Qin North normal fault zone. The valley is primarily V-shaped and deeply eroded with a slope of more than 35°. This mountain range is primarily composed of Proterozoic and Mesozoic granite gneiss with a highly weathered rock surface. Colluvial derived from these units cover the slopes, which are subject to frequent shallow landslides and other mass movement processes triggered by precipitation (Peng et al.,

1992).

The Li Mountain Zone in the southeast which occupies 6.4% of the Xi'an region is fault block uplift. It belongs to the family of tectonic uplift block mountains, with mostly intermediate to low elevation peaks; this range is influenced by the Li and Lintong-Chang'an faults. The highest elevation is 1,296 m above mean sea level, which is over 800 m above the Wei River plain. The landform has high peaks in the central part from where streams originate (radial distribution). The average slope is 14° with a range of 64° to 9°. This tectonic unit is primarily composed of pre-cambrian metamorphic rocks and the surface is covered by Quaternary loess. Slip surfaces form easily at the junction of rock and soil, resulting in the formation of a debris landslide in this region.

The Loess Tableland zone which occupies 4.6% of the Xi'an region is also located in the southeast. This zone decreases in elevation from the southeast to the northeast. Streams flowing along the edge of this tableland have eroded the loess, resulting in the formation of steep slopes and a flat tableland surface. The average slope of the loess tablelands is 9° with a range from 61° (distributed along the edge of the tableland) to 0°. The altitude varies from 834 m to 404 m.

Quaternary loess accounts for all of the Malan and Lishi loess deposits. In addition, these Quaternary deposits are fragmented in distribution, both in the gully and on the slopes along the edge of the tableland. Because of its relatively loose texture, metastable strength characteristics, collapsibility, and unique jointing structure (Lei, 1991; Liao, 2007), this material is very susceptible to instability in this area.

The Wei River plain which occupies 38.8% of the Xi'an region is located in the north. It is a flat landform characterized by alluvial deposits with no landslide occurrences.

The Xi'an Region has a monsoon-influenced climate with a prominent peak in precipitation during summer and a dry season in winter. During the period from May to October, the region receives about 77 percent of its total annual precipitation (Liao, 2007). Based on the meteorological records (1980–2010), the average annual precipitation and monthly precipitation are 584.9 mm and 53.7 mm, respectively, and the maximum annual precipitation, monthly precipitation, and daily precipitation are, 1131.7 mm, 258.8 mm, and 72.3 mm, respectively. Unsurprisingly, 97.3% of landslide occurrences have also been concentrated in this 6-month period (Zhao, 1993; Liao, 2007).

Warm and humid air from the southeast as well as cold and dry air from the Mongolian Plateau influences the regional climate, resulting in a predominantly extra-tropical monsoon climate. A stationary cold front is observed during autumn every year, resulting in long periods of heavy precipitation which in turn often causes landslides.

3 Methodology

The most commonly used multivariate statistical approaches for predicting landslides are discriminant analysis and logistic regression. Among the wide range of statistical methods proposed in the assessment of landslide susceptibility, logistic regression analysis has been found to be one of the most reliable approaches (Dai et al., 2002; Ayalew and Yamagishi, 2005; Guzzetti et al., 2006; Lee, 2007; Lee and Pradhan, 2007; Bai et al., 2010, 2011; Baghem et al., 2012). The advantage of this model is that it can be used even if the basic assumption of normality of the variables has not been met (García-Rodríguez et al., 2008). Altogether, logistic regression is well suited for the analysis of a dependent variable that is either present or absent; it is a statistical method that predicts the probability of an event occurrence, and has been used in various studies to predict landslides (Piacentini et al., 2012).

Logistic regression is used to analyze the relationships between one dependent variable and several independent variables, creating a mathematical model that predicts the probability of occurrence of the dependent variable. We used logistic regression analysis in order to predict landslide occurrence in a particular area. This method assigns values of either 1 or 0 to each variable to analyze the probability of a landslide occurrence, and hence, these values correspond to landslide occurrence or non-occurrence, respectively.

In the case of landslide prediction, the objective of logistic regression is to develop a best-fitting model that describes the relationship between the dependent variable (Y) of landslide occurrence (or non-occurrence) and the independent variables (X_1, X_2,…, X_n) of the factors that influence landslide occurrences, such as slope angle, aspect, topographic wetness index (TWI), height difference, and slope shape. Logistic regression returns the probability of a positive binomial outcome in the form (García-Rodríguez et al., 2008; Bai et al., 2010, 2011; Baghem et al., 2012; Piacentini et al., 2012):

$$Y = e^x/1 + e^x, \quad (1)$$

where, Y is the probability of a landslide occurrence in percent; x is $\beta_0 + \beta_1X_1 + \beta_2X_2 + \ldots + \beta_iX_i$; β_i is the i^{th} coefficient of the logistic regression model and is X_i's contribution to the model; and X_i (i = 1, 2,…, n) represent the influencing factors or independent variables of landslide events. Five independent variables of terrain factors describing the slope gradient, TWI, height difference, profile curvature, and slope aspect were evaluated.

The advantage of the logistic regression approach is that it does not require or assume linear dependencies between the dependent variable and the independent variables involved. The corresponding coefficients can be estimated through the maximum likelihood criterion, by which the

more likely unknown factors can be estimated. In this study, the independent variables for the geographical data used in this study were included in the GIS environment followed by a logistic regression analysis using SPSS, the flowchart of landslide susceptibility analysis shows in Fig. 3.

4 Data analysis and landslide distribution

Landslide occurrences were recorded via field investigations in this study and by the Geology Environmental Monitoring Station of Xi'an during the period 1980–2010. The landslide database compiled for this analysis includes information on 278 landslides that occurred in this region during the period 1980–2010 (Table 1, Fig. 2), including 49 landslides in the Loess Tableland, 63 landslides in the Li Mountain, and 166 landslides in the Qin Mountain (Table 1).

Two factors are important when conducting landslide assessments; causal factors and modeling methods (Dai et al., 2002). Landslides result from the relationships of complex and sometimes unknown factors that differ by the type of geological movement and vary according to the physical environment. Based on field geomorphological and geological investigations coupled with the analysis of landslides, a general explicit phenomenon was established to characterize landslides in the Xi'an Region. The major features of these phenomena are (i) the sliding surfaces are generally located at the lower boundary of the regolith, about 2 m below the surface in the Qin Mountain, and 8−10 m below the surface in the Li Mountain, (ii) the landslides in the loess tableland are primarily distributed along the edge, (iii) landslide occurrences are primarily controlled by topography due to the unique geology of the loess tableland, however, the regolith landslides are dominant in the mountain ranges. The landslide stability is affected by the slope angle, hydrological characteristics, potential energy, and the slope profile associated with landform according to the landslide stability equation (Fernandes et al., 2004; Mansouri Daneshvar and Bagherzadeh, 2011; Piacentini et al., 2012). Therefore, the slope angle, hydrological characteristics (TWI), potential energy (height difference), and the slope profile (profile curvature and slope aspect) were selected for the analysis of the relationship between topography and landslide occurrences (Fernandes et al., 2004; Piacentini et al., 2012). These variables were used to determine the dependent variable of occurrence or nonoccurrence of landslides within an individual grid cell with 25 m resolution on

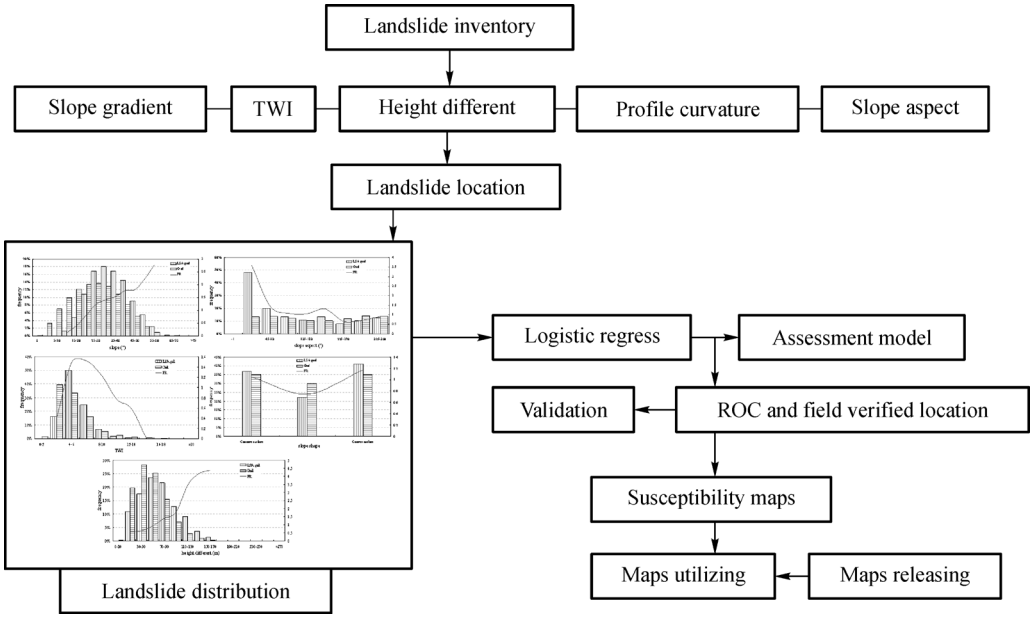

Fig. 3 Flowchart of landslide susceptibility analysis

Table 1 The landslide frequencies in the three sub-regions in Xi'an and their geological characteristics

Sub-region	Number of landslides	Geology
Loess Tableland	49	Loess deposits.
Li Mountain	63	1−2 layers of loess on the surface, overlying mudstone and conglomerate rock.
Qin Mountain	166	Metamorphic rocks.

1:50,000 scale topographic map. The five respective topographical parameter sets that were constructed considering appropriate conditioning factors and sampling strategies and are discussed below.

4.1 Slope gradient

Field surveys show that the slope gradient is one of the most important topographical factors influencing landslide occurrences. In general, a higher slope gradient corresponds to a high possibility of slope failure. In addition, the gradient affects the infiltration and runoff rates as well as the thickness of the regolith layer and other parameters (Montgomery and Dietrich, 1994; Fernandes et al., 2004). Its value may be calculated from the DEM by the inclination computational method using a 3×3 moving window. As a result, the values of the slope angles are divided into classes in increments of 5° (i.e., 0°–5°, 5°–10°,…, 70°–75°, and > 75°) (Fig. 4).

Figure 4 indicates the density of landslide distribution in slopes of each of the three regions. Correlation analysis revealed that the highest density of landslides (51.81%) was in the slope range of 25°−40° (Fig. 4(a)) in the Qin Mountain, while 49.21% of landslides occurred in the slope range of 15°−25° (Fig. 4(b)) in the Li Mountain, and 69.39% of landslides occurred in the slope range of 20°−40° (Fig. 4(c)) in the loess tableland. Meanwhile, frequency distributions of landslides indicate that the probability of landslide occurrence increased with slope angle up to a point particularly at slopes above 25° in the Qin Mountain, 15° in the Li Mountain, and 20° in the Loess Tableland. At lower slope gradients, the density of landslides is low because the terrain is gentle and covered with thick colluvium and/or residual soils which require higher water levels to initiate slope failures. Meanwhile, at very high slope gradients, the density of landslides is also low because the terrain is very steep with a small amount of colluvium. The most common slope range varies from 28° in the Qin Mountain to 22° in the Li Mountain and 29° in the Loess Tableland.

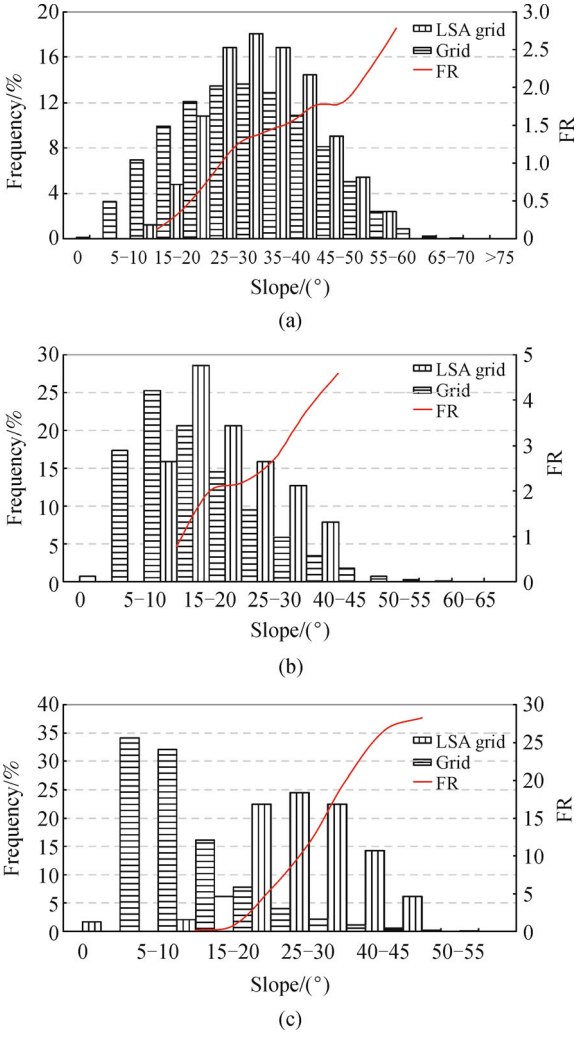

Fig. 4 Frequency distribution of landslides in different classes of slope gradients in the three sub-regions of Xi'an. LSA grid (%): percent of each grid affected by landslides; Grid (%): percentage of grids in the domain; FR: percent of total grids affected by landslides; (a) Qin Mountain; (b) Li Mountain; (c) Loess Tableland.

4.2 Slope aspect

The aspect of a slope can influence moisture retention and vegetation cover, which then affects soil strength and landslide occurrences. It also affects the infiltration and runoff rates (Wieczorek et al., 1997). Aspect can be defined as the slope direction which identifies the downslope direction of the maximum rate in change of elevation (Fernandes et al., 2004) and calculated in compass degrees (from −1 to 360), based on the surface tools in ARCGIS. Zero, 90, 180, and 270 degrees indicate north, east, south, and west, respectively.

Within the sub-regions, the majority of landslides occurred on the northeast slopes of the Qin Mountain (68.07%), on the northwest and southeast slopes of the Li Mountain (42.6%), and on the northwest and southwest slopes of the Loess Tableland (40.82%). Analyses of landslide frequency distributions reveals that slope angles in the range 0°−45° in the Qin Mountain, 135°−180° in the Li Mountain, and 180°−225° in the Loess Tableland correspond to high probabilities of landslide occurrences (Fig. 5). This distribution phenomenon was primarily affected by the orientation of the mountain ranges; the Qin Mountain runs from west to east, while the Li Mountain and loess tableland run from the SE to the NW.

4.3 Topographic Wetness Index (TWI)

The topographic wetness index, developed by Beven and Kirkby (1979) within the runoff model, affects the spatial distribution of soil moisture by influencing the ground-

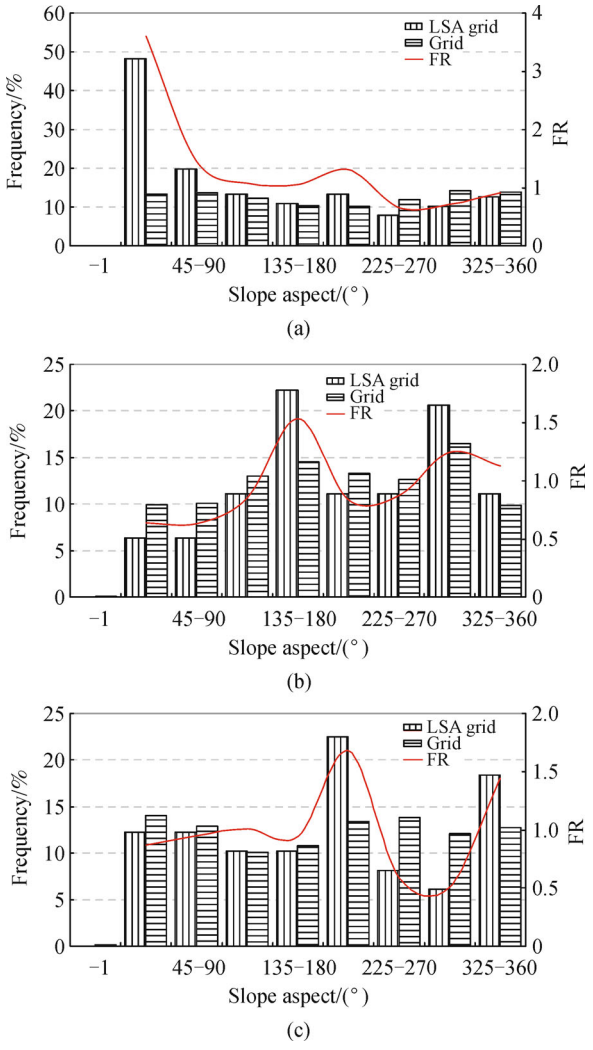

Fig. 5 Frequency distribution of landslides in different slope aspect classes in the three sub-regions of Xi'an. LSA grid (%): percent of each grid affected by landslides; Grid (%): percent of grids in the domain; FR: grids affected by landslides as a percentage of all grids; (a) Qin Mountain; (b) Li Mountain; (c) Loess Tableland.

water flow as it follows surface topography. It can be defined as:

$$\mathrm{TWI} = \ln(\alpha/\tan\beta), \tag{2}$$

where, α is the local upslope area draining through a certain point per unit contour length, and $\tan\beta$ is the local slope. Some studies have indicated that landslides are primarily distributed along slopes with high TWI and gradients, because a high TWI encourages water collection and hence higher soil moisture (Yilmaz, 2009; Regmi et al., 2010). This consequently reduces the strength of rock and soil on the slope (Yilmaz, 2009). TWI was calculated using the raster calculation tools.

The highest frequency of landslides in each sub-region occurred in the TWI classes of 4−6 (50%) in the Qin Mountain, 4−6 (46%) in the Li Mountain, and 4−6 (46.94%) in the Loess Tableland, indicating that the highest TWI does not correspond to the greatest landslide activity. The frequency distributions indicate that the highest probabilities of landslide occurrences are linked with intermediate values of TWI. TWI values lower than 4 are present in steep and rocky regions, whereas the values higher than 7 correspond to relatively flat and gentle topography (Yilmaz, 2009) (Fig. 6).

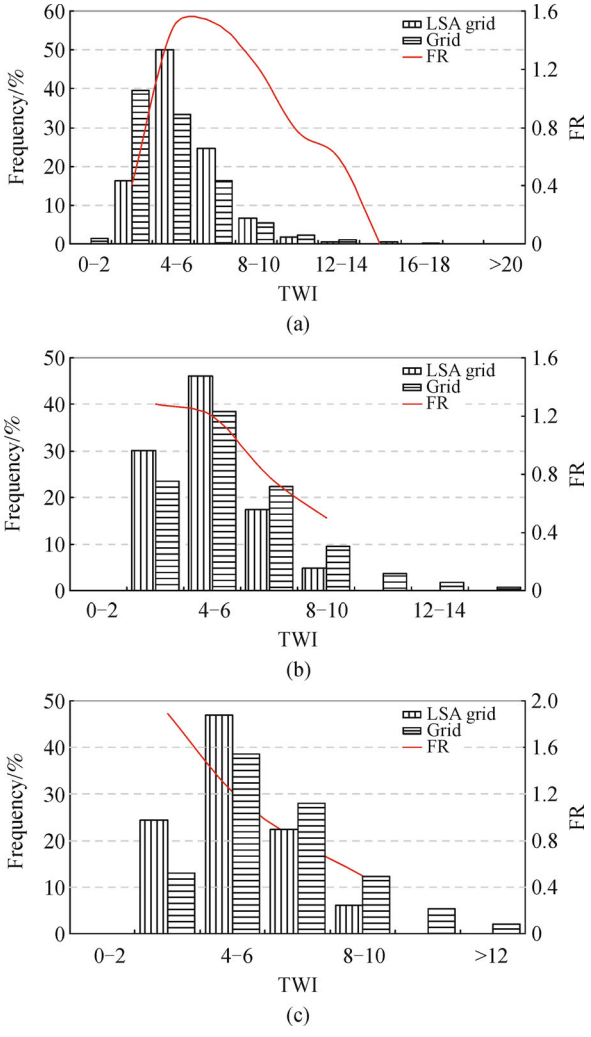

Fig. 6 Frequency distribution of landslides in different TWI classes in the three sub-regions of Xi'an. LSA grid (%): percent of each grid affected by landslides; Grid (%): percent of grids in the domain; FR: grids affected by landslides as a percentage of all grids; (a) Qin Mountain; (b) Li Mountain; (c) Loess Tableland.

4.4 Profile curvature

This represents curvature in the vertical plane parallel to the slope direction (Wilson and Gallant, 2000). It measures the rate of change in the slope, and therefore, influences the flow velocity of water draining across the surface. This in turn influences erosion and the movement of sediments

(Kayastha, 2012). Profile curvature can be calculated by subtracting the mean value of the DEM from the true value of the DEM using a moving window of 3 × 3 points. Positive values indicate convex–upward surfaces and negative values indicate convex–downward surfaces, while a value of zero indicates that the slope is planar (Wilson and Gallant, 2000). Therefore, the values of curvature were classified into three classes of surfaces, that is, concave, planar, and convex.

Within the three sub-regions of interest, landslide occurrences are abundant at locations with convex (40.96%) and concave surfaces (36.75%) in the Qin Mountain, planar surfaces (42.86%) in the Li Mountain, and convex (40.82%) and planar (34.70%) surfaces in the Loess Tableland. Frequency ratio values greater than 1 are present at concave and convex surfaces in the Qin Mountain, concave surfaces in the Li Mountain, and convex surfaces in the Loess Tableland; these surfaces are more susceptible to landslide occurrences (Fig. 7).

4.5 Height difference

Height difference is a measure of the potential gravitational energy of the landslide. In general, an increased height difference corresponds to an increased possibility of failure due to an increase in the sliding force (Fernandes et al., 2004). It can be calculated by subtracting the minimum value of the DEM from the maximum value of the DEM using a moving window of 3 × 3 points.

Within the three sub-regions, the majority of landslides occurred in the height difference range of 50−90 m (45.18%) in the Qin Mountain, 10−70 m (87.30%) in the Li Mountain, and 10−30 m (44.90%) in the Loess Tableland (Fig. 8). Frequency ratio analyses revealed that landslide frequencies increase proportionately with the height difference in the Qin and Li Mountains, but the frequency began to drop off at height differences exceeding 60 m. This is because the land with height differences exceeding this value are generally used for terraced cultivation.

4.6 Construction of prediction model

The logistic regression model estimates coefficients for each of the parameters using the mean and maximum likelihood method instead of the least squares method that is normally used in linear regression (Ayalew and Yamagishi, 2005; Lee, 2007; Lee and Pradhan, 2007; Bai et al., 2011). The precision of maximum likelihood increases with sample size. However, in order to construct a dataset with homogeneous cells to find out the presence/absence of landslides, an equal number of points free from the DEM map were randomly extracted from the whole dataset and used in the "training" phase of the LR analysis (García-Rodríguez et al., 2008; Yilmaz, 2009).

The five aforementioned parameters were selected for performing the logistic regression. The established relationships between landslides and the various influencing topographic factors are listed as follows; x_1 is slope gradient, x_2 is profile curvature, x_3 is height difference, x_4 is slope aspect, x_5 is TWI.

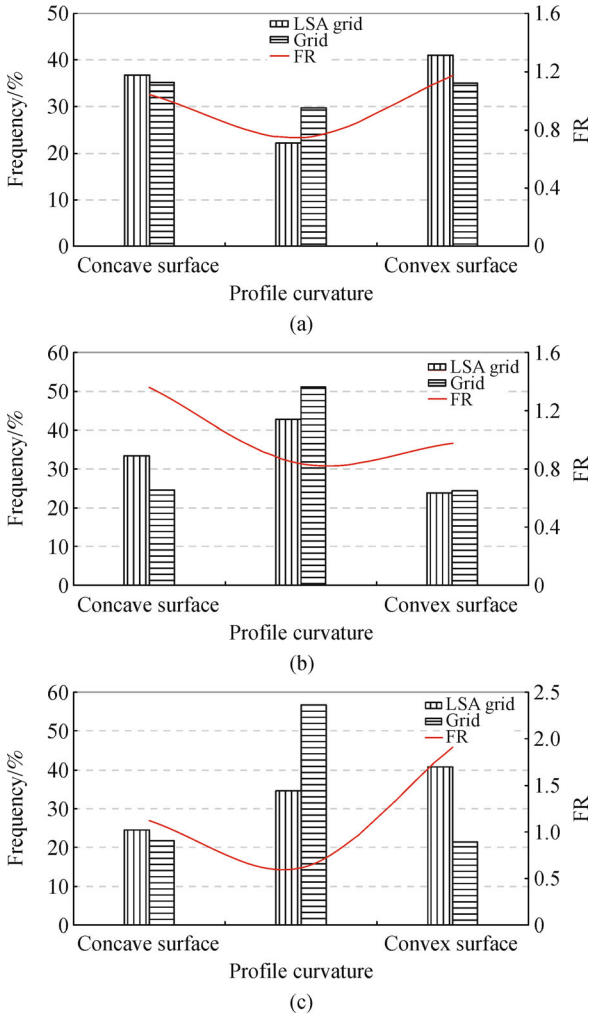

Fig. 7 Frequency distribution of landslides in different profile curvature classes in the three sub-regions. LSA grid (%): percent of each grid affected by landslides; Grid (%): percent of grids in the domain; FR: grids affected by landslides as a percentage of all grids; (a) Qin Mountain; (b) Li Mountain; (c) Loess Tableland.

In this model, the GIS software was used for the processing and management of data related to individual factors, while statistical analysis by logistic regression was performed using SPSS after exporting the data to suitable exchange formats. The methodology used for the logistic regression model is based on quantitative variables; however, it is also possible to use qualitative variables in the model by creating layers of binary values (dummy variables) for each class of an independent qualitative parameter (Lee and Min, 2001; Dai and Lee, 2002; Ayalew and Yamagishi, 2005).

The logistic regression model was constructed using the

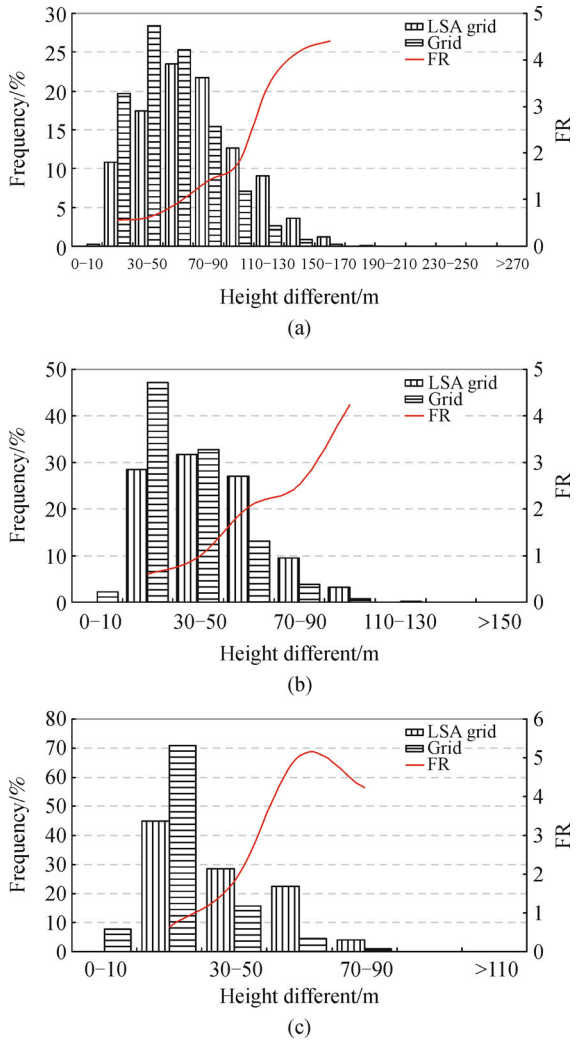

Fig. 8 Frequency distribution of landslides in different height difference classes in the three sub-regions of Xi'an. LSA grid (%): percent of each grid affected by landslides; Grid (%): percent of grids in the domain; FR: grids affected by landslides as a percentage of all grids; (a) Qin Mountain; (b) Li Mountain; (c) Loess Tableland.

entire dataset. Using the "logit" function, we calculated the probability that each parameter contributed to landslide susceptibility based on Eq. (1). Here, the coefficients of the logit function are as follows;

The logit function for the Qin Mountain is

$$Y = -4.181 + 0.187 \times SG + 0.016 \times PC - 0.026 \times HD - 0.001 \times SA + 0.240 \times TWI; \quad (3)$$

the logit function for the Li Mountain is

$$Y = -6.276 + 0.139 \times SG + 0.100 \times PC - 0.006 \times HD + 0.005 \times SA + 0.558 \times TWI; \quad (4)$$

the logit function for the Loess Tableland is

$$Y = -6.297 + 0.231 \times SG - 0.033 \times PC - 0.019 \times HD + 0.002 \times SA + 0.367 \times TWI, \quad (5)$$

where, *SG* is the slope gradient, *PC* is the profile curvature, *HD* is the height difference, and *SA* is the slope aspect.

As shown in Table 2, a good correlation was found between the percentage of actual landslides and their predicted probabilities. The influencing factors, including slope gradient, profile curvature, height difference, slope aspect, and TWI, show a test accuracies of above 84% of the classifications in the three models, indicating that the model predictions are consistent with field observations.

The performance of the training dataset was judged based on the ROC curve (Swets, 1988). The ROC curve is a plot of the sensitivity (proportion of true positives) of the model's prediction versus the complement of its specificity (proportion of false positives), at a series of thresholds for a positive outcome. Sensitivity is the probability that a mapping unit with landslides is correctly classified, and is plotted on the *y*-axis in an ROC curve; sensitivity is the true positive rate (Nefeslioglu et al., 2010). Specificity is the probability that a mapping unit with zero landslide occurrences is correctly classified; 1-specificity is the false

Table 2 Correlation between the percentage of actual landslides and the predicted probability of landslides

			Predicted		Percentage accuracy/%
			0	1	
(a) Qin Mountain	Observed	0	55	8	87.30
		1	10	53	84.12
	Overall percentage				85.71
(b) Li Mountain	Observed	0	43	6	87.75
		1	4	45	91.84
	Overall percentage				89.75
(c) Loess Tableland	Observed	0	150	16	90.36
		1	13	153	92.17
	Overall percentage				91.26

positive rate and is mapped along the *x*-axis of the curve. The area under the curve represents the probability of the landslide susceptibility value for a landslide mapping unit calculated by the model's exceeding the result for a randomly chosen no-landslide-occurrence mapping unit. The ROC curve for the model developed is indicated in Fig. 9, and the areas obtained under the curve were 0.86, 0.84, and 0.92 in the Qin Mountain, Li Mountain, and Loess Tableland, respectively. This confirms the robustness of the constructed model.

As discussed above, the relative importance of the independent variables can be expressed by the regression coefficient, highlighting the causal factors and variables that are most strongly related to the occurrence of landslides. Among these, TWI and slope gradient appear to be the most strongly related to slope failure occurrences in all of the three sub-regions. However, classes such as height difference and slope aspect in the Qin Mountain, height difference in the Li Mountain, and profile curvature and height difference in the Loess Tableland indicated negative regression coefficients, suggesting that they actually protect against landslide occurrences.

Using the regression logistic model, five classes of susceptibilities were identified and mapped; (i) very low (0−0.2), (ii) low (0.2−0.4), (iii) medium (0.4−0.6), (iv) high (0.6−0.8), and (iv) very high (0.8−1). The landslide distributions among the five classes in each of the three sub-regions are shown in Table 3.

Figure 10 indicates the distribution of modeled landslide susceptibilities in the Qin Mountain, Li Mountain, and Loess Tableland. The distribution of landslide susceptibility probability in the Qin Mountain indicates that the hazards with very high probability are concentrated in intermediate altitudes. Historical observations reveal that 76.8% of the landslides occurred within the very high and high susceptibility classes (Fig. 10(a)). The distribution of landslide susceptibility probability in the Li Mountain reveals that the hazards with very high probability are concentrated along the Wei River and the north slopes of the mountains. Historical observations reveal that 84.2% of the landslides occurred within the very high, high, and medium susceptibility classes. Furthermore, the very high class of susceptibilities which accounted for only 13.15% of the total study area was responsible for approximately 39.7% of all observed landslides (Fig. 10(b)). Finally, with regard to the Loess Tableland, landslides in the high susceptibility class were concentrated along the north-east and north-west edges of the study area and along the

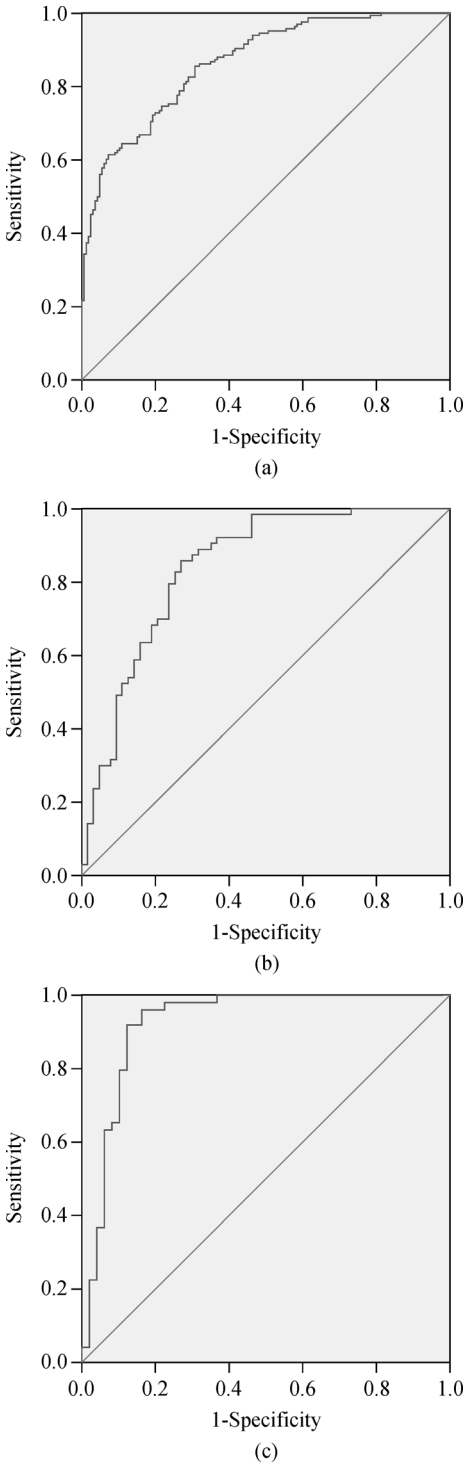

Fig. 9 ROC curve. Results are described in the text. (a) Qin Mountain; (b) Li Mountain; (c) Loess Tableland.

Table 3 Landslide distributions in different susceptibility classes

	Qin Mountain	Li Mountain	Loess Tableland
Very low class	15.24%	15.55%	63.07%
Low class	18.24%	29.13%	19.10%
Medium class	17.44%	23.56%	8.39%
High	20.59%	18.62%	5.08%
Very high class	28.48%	13.15%	4.35%

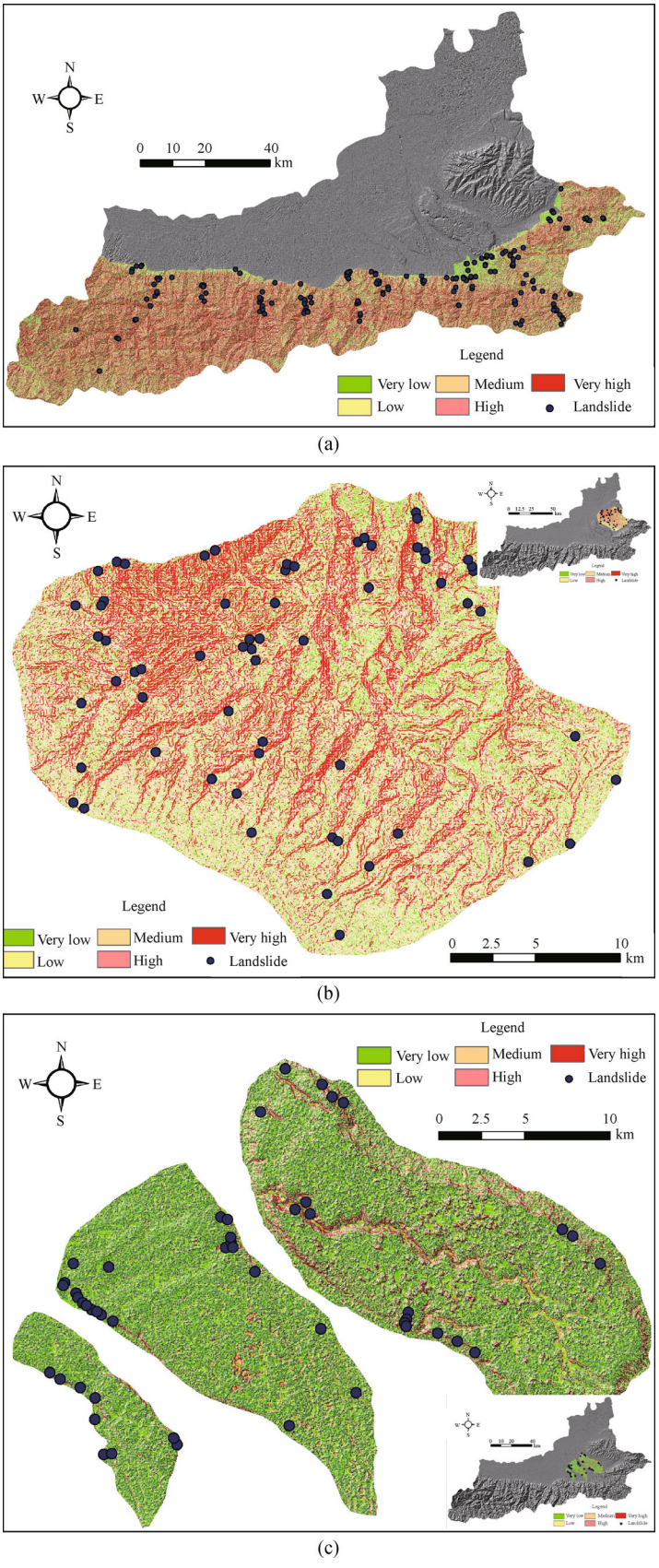

Fig. 10 Susceptibility map generated from the logistic regression model for the three sub-regions in Xi'an, China. (a) is the Qin Mountain; (b) is the Li Mountain; (c) is the Loess Tableland.

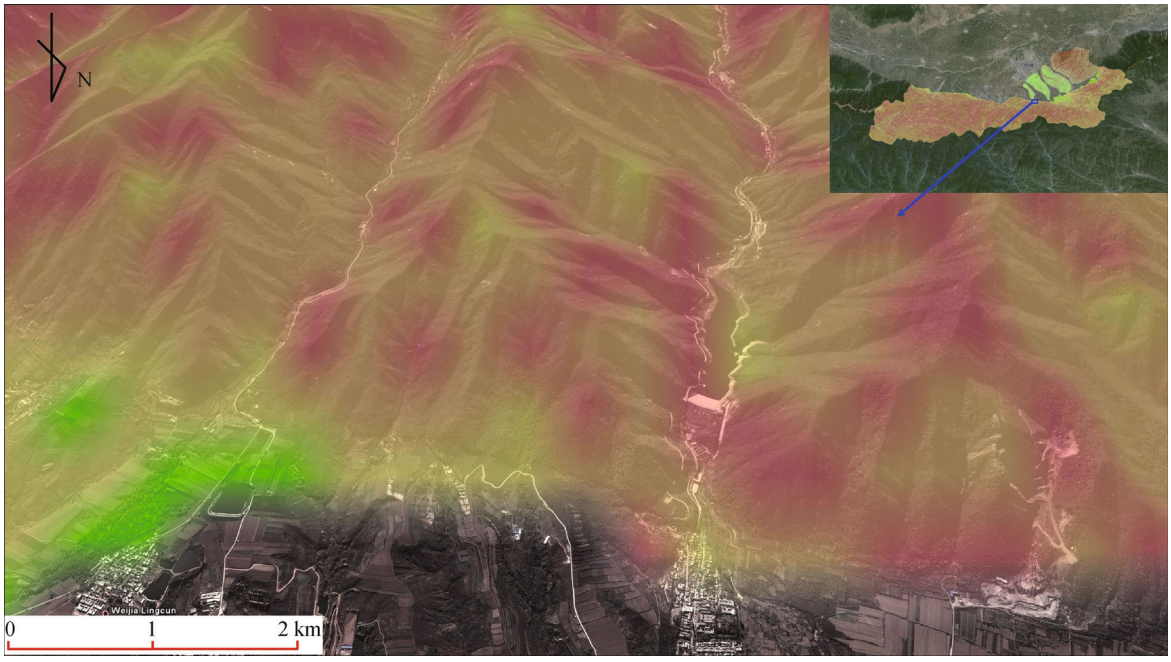

Fig. 11 Susceptibility map converted to a KML shape overlaid on Google Earth.

Qingyu Gully in the Bailu Tableland. Historical data revealed that 82.9% of the landslides in this sub-region were in the very high and high susceptibility classes. Furthermore, the very high class which occupies only 4.35% of the total study area contains approximately 54.1% of all observed landslides (Fig. 10(c)).

Many areas selected for future construction work are located in certain zones of the high susceptibility areas of our model; however, no active phenomena have yet been observed in these zones. To avoid damage from landslides, all plans for land use should avoid any infrastructure installation or construction activity in the very high, high, and medium susceptibility classes. Moreover, the susceptibility maps can be exported to a Keyhole Markup Language (KML) shape, which can be opened using Google Earth. Figure 11 indicates the KML shapes for the landslide susceptibility map of the Qin Mountain. These shapes are easy for the general public to read and comprehend when planning construction projects.

5 Conclusions

This research shows the distribution of landslides and the application of logistic regression to map landslide susceptibility in the Xi'an Region. Five surface topographical factors, namely, slope gradient, TWI, height difference, profile curvature, and slope aspect, were selected to study their influence on landslide distributions in the three sub-regions that witnessed the landslides; Qin Mountain, Li Mountain, and Loess Tableland. The logistic regression model revealed that the influence of these factors and the classes responsible for the highest landslide frequency were specific to each sub-region. According to the regression coefficients, TWI and slope gradient have a stronger influence on slope failure occurrences than the other three factors in all of the three sub-regions. Since the model was in agreement with historical observations, the maps presented in this study can be used by local as well as regional governments to predict the risks of future landslides.

Landslide susceptibility can be assessed using different methods based on GIS technology. During last two decades or so, many research studies have focused on addressing the difficulties in assessing landslide susceptibility. However, converting susceptibility maps to a format which can be easily understood by a non-expert person remained a challenge, and this must be taken into account while preparing landslide susceptibility maps irrespective of method used.

Acknowledgements We are grateful to the editors who devoted much time in correcting this manuscript and for their valuable suggestions and constructive comments. We would also like to express our gratitude to the academic and technical staff of the Institute of Geo-hazards Mitigation and Research of Chang'an University, China. This work was financially supported by the National Basic Research Program of China (No. 2014CB744703), the National Natural Science Foundation of China (Grant Nos. 41202244 and 41130753), and the Fundamental Research Funds for the Central Universities (2013G1261063).

References

Ayalew L, Yamagishi H (2005). The application of GIS-based logistic

regression for landslide susceptibility mapping in the the Kakuda-Yahiko Mountains, Central Japan. Geomorphology, 65(1–2): 15–31

Baghem M, Chouabi B, Abdel M, Demdoum C, Abdeslem D (2012). Geologic, topographic and climatic controls in landslide hazard assessment using GIS modeling: a case study of Souk Ahras region, NE Algeria. Quaternary International, 302(17): 224–237

Bai S, Lu G, Wang J, Zhou P, Ding L (2011). GIS-based rare events logistic regression for landslide-susceptibility mapping of Lianyungang, China. Environment Earth Science, 62(1): 139–149

Bai S B, Wang J, Lu G, Zhou P, Hou S S, Xu S N (2010). GIS-based logistic regression for landslide susceptibility mapping of the Zhongxian segment in the Three Gorges area China. Geomorphology, 115(1–2): 23–31

Beven K J, Kirkby M J (1979). A physically based, variable contributing area model of basin hydrology. Hydrol Sci Bull, 24(1): 43–69

Cui P, Zhou G G D, Zhu X H, Zhang J Q (2012). Scale amplification of natural debris flows caused by cascading landslide dam failures. Geomorphology, 123: 1–17

Cui P, Zou Q, Xiang L Z, Zeng C (2013). Risk assessment of simultaneous debris flows in mountain townships. Prog Phys Geogr, 37(4): 516–542

Dai F C, Lee C F (2002). Landslide characteristics and slope instability modeling using GIS, Lantau Island, Hong Kong. Geomorphology, 42 (3–4): 213–228

Dai F C, Lee C F, Ngai Y Y (2002). Landslide risk assessment and management: an overview. Eng Geol, 64(1): 65–87

Dai F C, Lee C F, Zhang X H (2001). GIS-based geo-environmental evaluation for urban land-use planning: a case study. Eng Geol, 61 (4): 257–271

Ermini L, Catani F, Casagli N (2005). Artificial Neural Networks applied to landslide susceptibility assessment. Geomorphology, 66(1–4): 327–343

Fell R, Corominas J, Bonnard C, Cascini L, Leroi E, Savage W Z (2008). Guidelines for landslide susceptibility, hazard and risk zoning for land use planning. Eng Geol, 102(3–4): 85–98

Fernandes N F, Guimarães R F, Gomes R A T, Vieira B C, Montgomery D R, Greenberg H (2004). Topographic controls of landslides in Rio de Janeiro: field evidence and modeling. Catena, 55(2): 163–181

García-Rodríguez M J, Malpica J A, Benito B, Díaz M (2008). Susceptibility assessment of earthquake-triggered landslides in El Salvador using logistic regression. Geomorphology, 95(3–4): 172–191

Guzzetti F, Peruccacci S, Rossi M, Stark C P (2008). The rainfall intensity–duration control of shallow landslides and debris flows: an update. Landslides, 5(1): 3–17

Guzzetti F, Reichenbach P, Ardizzone F, Cardinali M, Galli M (2006). Estimating the quality of landslide susceptibility models. Geomorphology, 81(1–2): 166–184

Iverson R M (1997). The physics of debris flows. Rev Geophys, 35(3): 245–296

Kayastha P (2012). Application of fuzzy logic approach for landslide susceptibility mapping in Garuwa sub-basin, East Nepal. Front Earth Sci, 6(4): 420–432

Keefer D K, Wilson R C, Mark R K, Brabb E E, Brown W. M (1987). Real-time landslide warning during heavy rainfall. Science, 238(13): 921–925

Lee S (2007). Comparison of landslide susceptibility maps generated through multiple logistic regression for three test areas in Korea. Earth Surface Processes and Landforms, 32(14): 2133–2148

Lee S, Min K (2001). Statistical analysis of landslide susceptibility at Yongin, Korea. Environment Geology, 40(9): 1095–1113

Lee S, Pradhan B (2007). Landslide hazard mapping at Selangor, Malaysia using frequency ratio and logistic regression models. Landslides, 4(1): 33–41

Lei X Y (1991). The stability of loess landslides on the edges of the bailuyuan tableland, Xi'an and their relationship with human activities. Geology Review, 37(3): 258–264 (in Chinese)

Li Y S (1992). Xi'an Crack and the Weihe River Basin Active Fault Research. Beijing: Seismological Press (in Chinese)

Liao W D (2007). Analysis of Characteristic and cause of formation of landslides at bailuyuan. Journal of Disaster Prevention and Mitigation Engineering, 27(1): 80–85 (in Chinese)

Liu X L, Yu C J, Shi P J, Fang W H (2012). Debris flow and landslide hazard mapping and risk analysis in China. Front Earth Sci, 6(3): 306–313

Mansouri Daneshvar M R, Bagherzadeh A (2011). Landslide hazard zonation assessment using GIS analysis at Golmakan Watershed, northeast of Iran. Front Earth Sci, 5(1): 70–81

Montgomery D R, Dietrich W E (1994). A physically based model for the topographic control on shallow landsliding. Water Resources Research, 30: 1153–1171

Nandi A, Shakoor A (2010). A GIS-based landslide susceptibility evaluation using bivariate and multivariate statistical analyses. Eng Geol, 110(1–2): 11–20

Nefeslioglu H A, Sezer E, Gokceoglu C, Bozkir A S, Duman T Y (2010). Assessment of landslide susceptibility by decision trees in the metropolitan area of Istanbul, Turkey. Mathematical Problems in Engineering, 90(105): 89–93

Peng J B, Zhang J, Su S R, Mi F S (1992). Active Faults and Geological Hazards in Wei Basin. Xi'an: Northwest University Press (in Chinese with English Abstract)

Piacentini D, Troiani F, Soldati M, Notarnicola C, Savelli D, Schneiderbauer S S C, Strada C (2012). Statistical analysis for assessing shallow-landslide susceptibility in South Tyrol (south-eastern Alps, Italy). Geomorphology, 151–152: 196–206

Regmi N R, Giardino J R, Vitek J D (2010). Modeling susceptibility to landslides using the weight of evidence approach: Western Colorado, USA. Geomorphology, 115(1–2): 172–187

Swets J A (1988). Measuring the accuracy of diagnostic systems. Science, 240(4857): 1285–1293

Tang C, van Asch T W J, Chang M, Chen G Q, Zhao X H, Huang X C (2012). Catastrophic debris flows on 13 August 2010 in the Qingping area, southwestern China: the combined effects of a strong earthquake and subsequent rainstorms. Geomorphology, 139 − 140: 559–576

Wieczorek G F, Mandrone G, DeCola L (1997). The influence of hillslope shape on debris-flow initiation. In: Chen C L, ed. Debris-Flow Hazards Mitigation: Mechanics, Prediction, and Assessment. California: American Society of Civil Engineers, 21–31

Wilson J P, Gallant J C (2000). Terrain Analysis. Principles and Applications. New York: Wiley, 113–127

Xu C, Xu X W, Dai F C, Saraf A K (2012). Comparison of different

models for susceptibility mapping of earthquake triggered landslides related with the 2008 Wenchuan earthquake in China. Comput Geosci, 46: 317–329

Xu C, Xu X W, Dai F C, Wu Z D, He H L, Shi F, Wu X Y, Xu S N (2013). Application of an incomplete landslide inventory, logistic regression model and its validation for landslide susceptibility mapping related to the May 12, 2008 Wenchuan earthquake of China. Nat Hazards, 68(2): 883–900

Xu Q, Fan X M, Huang R Q, Yin Y P, Hou S S, Dong X J, Tang M G (2010). A catastrophic rockslide-debris flow in Wulong, Chongqing, China in 2009: background, characterization, and causes. Landslides, 7(1): 75–87

Yilmaz I (2009). Landslide susceptibility mapping using frequency ratio, logistic regression, artificial neural networks and their comparison: a case study from Kat landslides (Tokat-Turkey). Comput Geosci, 35 (6): 1125–1138

Yune C Y, Chae Y K, Paik J, Kim G, Lee S W, Seo H S (2013). Debris flow in metropolitan area-2011 Seoul debris flow. Journal of Mountain Science, 10(2): 199–206

Zhao F S (1993) Features and occurring conditions of the bailuyuan slope failures, Xi'an. Journal of Xi'an College of Geology, 15(4): 167–171 (in Chinese)